

# Distance protection performance under inter-circuit faults on double-circuit transmission line

**Abstract.** Performance of distance protection of a double-circuit power transmission line under inter-circuit faults is analysed. A new algorithm for fault-loop impedance measurement designed for such faults is presented. Selected results of evaluation of the developed algorithm and its comparison with the algorithm designed for standard faults are included and discussed.

**Streszczenie.** Przeanalizowano działanie zabezpieczenia odległościowego dwutorowej linii elektroenergetycznej podczas zwarć między torami linii. Zaprezentowano nowy algorytm pomiaru impedancji pętli zwarciowej, przeznaczony dla tych zwarć. Przedstawiono i omówiono wybrane rezultaty testowania opracowanego algorytmu i jego porównania z algorytmem zaprojektowanym dla zwarć standardowych. (Działanie zabezpieczenia odległościowego podczas zwarć między torami na dwutorowej linii przesyłowej).

**Keywords:** transmission network, double-circuit line, inter-circuit fault, distance protection.

**Słowa kluczowe:** sieć przesyłowa, linia dwutorowa, zwarcie między torami, zabezpieczenie odległościowe.

## Introduction

This paper deals with distance protection of double-circuit transmission lines [1, 2, 3]. Such lines are constructed mainly due to constraints in obtaining new right-of-ways and are very common in power networks. Two three-phase circuits are arranged on the same tower and due to nearness of both circuits the magnetic coupling of them has to be taken into account. A current flowing in one circuit influences a voltage profile in the other circuit of a double-circuit line, and vice versa. The considerations are limited here to transposed lines and thus the symmetrical components technique is applied. In relation to this technique one uses the zero-sequence mutual impedance ( $Z_{0m}$ ) for reflecting the mutual coupling effect. In turn, the mutual impedance for the positive- and negative-sequence as very small are usually neglected.

A distance protection is commonly applied for protecting power system elements, mainly for overhead lines [1, 2, 3]. A principle of this protection is very well established, however, there is still much room for research on the distance protection subject. As for example, great interest in operation of distance protection in power grids with integrated wind farms is lately observed [4]. Very important issue is related with influence of transformation of instrument transformers on distance protection operation [5]. With the aim of improving quality of distance protection some knowledge-based [6, 7] and probabilistic [8] techniques are proposed. The other aim of the research conducted lately is related to development of both the hardware [9] and software [10] tools for distance relays testing and verification of their operation. The research area for distance protection appears as very wide and contains also investigation on power swing blocking [11]. An effort is paid to fault identification in terms of fault detection, direction discrimination and phase selection, which are also related to some fault location techniques [12] as well.

Yet, the other branch of current research on distance protection is devoted to measurement of fault-loop impedance under specific fault conditions [13–16]. In particular, in [14, 15, 16] impedance measurement under inter-circuit faults on a double-circuit line has been considered. In [14, 15] a measurement algorithm together with some limited evaluation was presented. This paper continues this subject providing new, more general and clear, derivation of the fault-loop impedance measurement algorithm. As in [16], the generalized fault-loop model is utilized for that. This was done with the aim of obtaining the compact formula applicable for different fault types, i.e. only

with setting some coefficients dependent on fault type. Moreover, this paper, as its innovative contribution, presents evaluation of distance protection performance under inter-circuit faults. Namely, protective relay reach and speed of operation, considering both the new and traditional measurements, are determined for a typical MHO impedance characteristic.

Firstly, the traditional measurement algorithm for fault-loop impedance under standard faults is presented. Then, a new measurement algorithm designed for inter-circuit faults is derived. Sample results of an evaluation of the considered algorithms are presented and discussed.

## Distance protection designed for standard faults

A principle of standard distance protection designed for standard faults can be explained in relation to the scheme of Fig.1. It is assumed within this paper that both circuits (I and II) of a double-circuit line are terminated at common buses (SI–SII and RI–RII). This is considered as a basic mode of a line operation [17]. Let the circuit SI–RI is affected by a standard shunt fault (F) of different types (Table 1), while the remaining circuit SII–RII remains healthy. Both the circuits are protected with distance protection relays installed at both ends of the circuits (SI, SII, RI, RII) and for the sake of simplicity only one of them (RELAY<sub>SI</sub> installed at SI) is depicted in Fig.1.

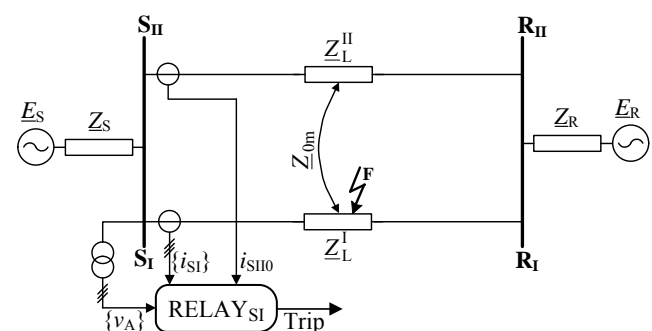


Fig.1. Distance protection of double-circuit line – the case of standard faults

Distance relays measure a fault-loop impedance with use of the fault-loop voltage and current (relaying voltage and current) composed accordingly to the recognized fault type. Considering typical, standard shunt faults (single phase faults and inter-phase faults) the fault-loop signals are composed as shown in Table 1 [17].

Table 1. Composition of fault-loop signals for standard faults

Fault type	Fault-loop: voltage ( $V_{FL}$ ), current ( $I_{FL}$ )
• <b>Phase-to-earth faults:</b> ph-E	$V_{FL} = V_{S1ph}$ , $I_{FL} = I_{S1ph} + \frac{Z_{0L} - Z_{1L}}{Z_{1L}} I_{S10} + \frac{Z_{0m}}{Z_{1L}} I_{S110}$
• <b>Inter-phase faults:</b> ph1-ph2, ph1-ph2-ph3, ph1-ph2-E, ph1-ph2-ph3-E	$V_{FL} = V_{ph1} - V_{ph2}$ , $I_{FL} = I_{ph1} - I_{ph2}$

ph1, ph2, ph3 – phases of three-phase system  
 ph – general description of faulted phase (for single-phase faults)  
 E – used for marking faults involving earth  
 $Z_{1L}$  – line impedance for positive- and negative-sequences  
 $Z_{0L}$ ,  $Z_{0m}$  – zero-, mutual zero-sequence line impedances  
 $V_{ph}$ ,  $I_{ph}$  – voltage, current from faulted phase 'ph'  
 $I_{S10}$  – zero-sequence current from faulted circuit SI–RI  
 $I_{S110}$  – zero-sequence current from healthy circuit SII–RII

### Inter-circuit faults

The schematic diagrams of faulted towers under different inter-circuit faults are shown in Fig.2. Two circuits of four-conductor bundles (phases:  $a^I, b^I, c^I$  and  $a^{II}, b^{II}, c^{II}$ ) together with a shielding earth wire (Sh E) are hung on a supporting tower. The models of the inter-circuit faults involving phases  $a^I, b^{II}$  are presented in Fig.3.

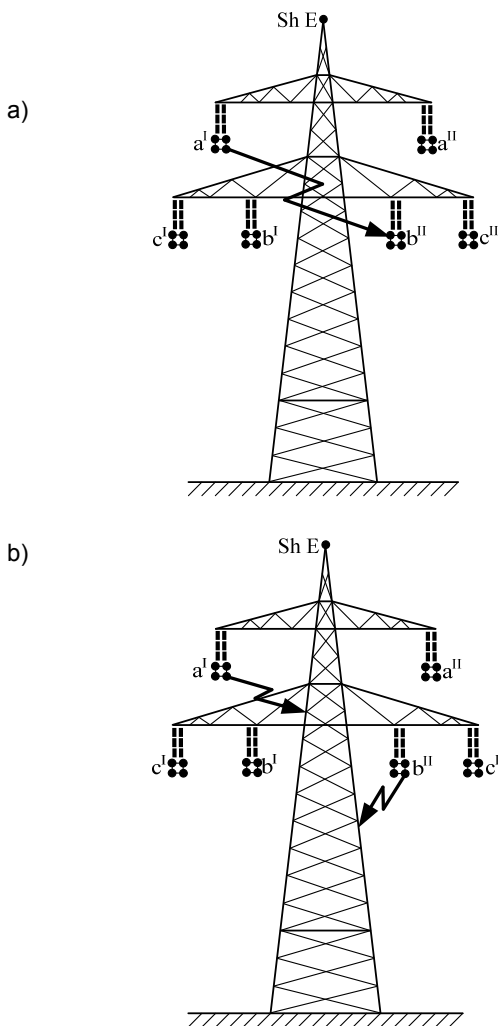


Fig.2. Schematic diagram of faulted tower under inter-circuit faults: a) phase-to-phase, b) phase-to-phase-to-earth

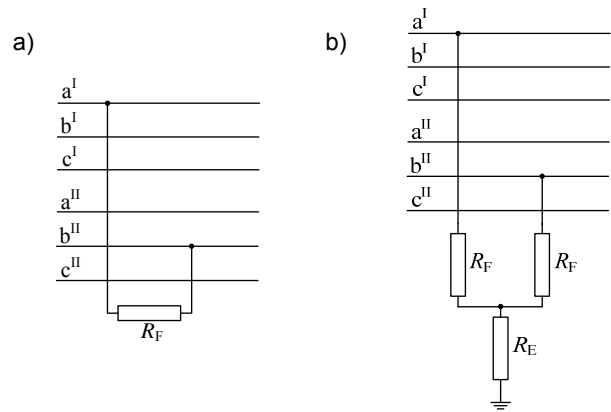


Fig.3. Models of inter-circuit faults: a) phase-to-phase, b) phase-to-phase-to-earth

### Distance protection designed for inter-circuit faults

In Fig.4 a principle of distance protection for a double-circuit line designed for inter-circuit faults is presented. In this case a relay (RELAYS) is supplied with a three-phase voltage  $\{v_S\}$  and three-phase current from the circuit to be protected  $\{i_{SI}\}$  and from the remaining circuit  $\{i_{SII}\}$ . Thus, complete measurements from one line end are utilized for protection.

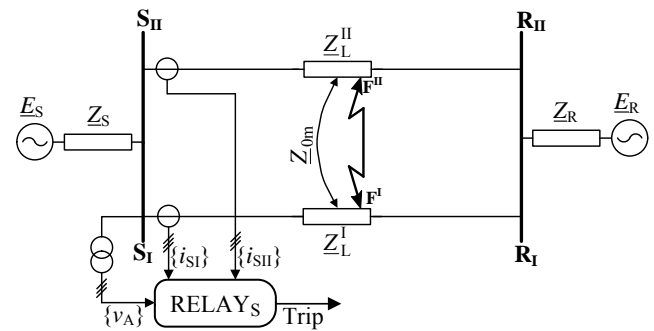


Fig.4. Distance protection of double-circuit line – the case of inter-circuit faults

Derivation of the measurement algorithm for fault-loop impedance under inter-circuit faults can be performed with use of equivalent circuit diagrams of faulted line for particular symmetrical components (Fig.5). It is marked there that the line circuits have different impedances, however, in practice due to identical geometry and conductors type these impedances are basically identical. Thus, in all further considerations it is assumed:

$$(1) \quad Z_{1L}^I = Z_{1L}^{II} = Z_{1L}$$

$$(2) \quad Z_{0L}^I = Z_{0L}^{II} = Z_{0L}$$

According to Fig.5 phasors of particular sequence components of voltage at the fault point  $F^I$  can be determined as follows:

$$(3) \quad V_{F1}^I = V_{S1} - d Z_{1L} I_{S1}^I$$

$$(4) \quad V_{F2}^I = V_{S2} - d Z_{1L} I_{S2}^I$$

$$(5) \quad V_{F0}^I = V_{S0} - d Z_{0L} I_{S0}^I - d Z_{0m} I_{S0}^{II}$$

where:

$d$  – distance to fault [p.u.], counted from buses SI–SII to fault points  $F^I, F^{II}$ .

Analogously one determines sequence voltages for the fault point  $F^{\text{II}}$ :

$$(6) \quad \underline{V}_{F1}^{\text{II}} = \underline{V}_{S1} - d\underline{Z}_{1L}^{\text{II}} \underline{I}_{S1}^{\text{II}}$$

$$(7) \quad \underline{V}_{F2}^{\text{II}} = \underline{V}_{S2} - d\underline{Z}_{1L}^{\text{II}} \underline{I}_{S2}^{\text{II}}$$

$$(8) \quad \underline{V}_{F0}^{\text{II}} = \underline{V}_{S0} - d\underline{Z}_{0L}^{\text{II}} \underline{I}_{S0}^{\text{II}} - d\underline{Z}_{0m}^{\text{II}} \underline{I}_{S0}^{\text{I}}$$

In order to formulate an algorithm for calculation of fault-loop impedance by adaptive distance protection under inter-circuit faults, the generalized fault-loop model [16] is stated:

$$(9) \quad \underline{V}_{\text{FL}}^{\text{I-II}} - R_F \underline{I}_F = 0$$

where:

$\underline{V}_{\text{FL}}^{\text{I-II}}$  – fault-loop voltage between the fault points:  $F^{\text{I}}$ ,  $F^{\text{II}}$ ,

$R_F$  – fault resistance,

$\underline{I}_F$  – fault path current (total fault current).

Fault-loop voltage involved in (9) can be composed as a difference of voltages from faulted phases at the fault points:  $F^{\text{I}}$ ,  $F^{\text{II}}$ . Using the weighting coefficients dependent on fault type [17] (Table 2) the fault-loop voltage is:

$$(10) \quad \underline{V}_{\text{FL}}^{\text{I-II}} = (\underline{a}_1^{\text{I}} \underline{V}_{F1}^{\text{I}} + \underline{a}_2^{\text{I}} \underline{V}_{F2}^{\text{I}} + \underline{a}_0^{\text{I}} \underline{V}_{F0}^{\text{I}}) - (\underline{a}_1^{\text{II}} \underline{V}_{F1}^{\text{II}} + \underline{a}_2^{\text{II}} \underline{V}_{F2}^{\text{II}} + \underline{a}_0^{\text{II}} \underline{V}_{F0}^{\text{II}})$$

where:

$\underline{V}_{F1}^{\text{I}}$ ,  $\underline{V}_{F2}^{\text{I}}$ ,  $\underline{V}_{F0}^{\text{I}}$  – sequence voltages defined in (3)–(5),

$\underline{V}_{F1}^{\text{II}}$ ,  $\underline{V}_{F2}^{\text{II}}$ ,  $\underline{V}_{F0}^{\text{II}}$  – sequence voltages defined in (6)–(8).

Table 2. Weighting coefficients for different inter-circuit faults

Fault type	Circuit I			Circuit II		
	$\underline{a}_1^{\text{I}}$	$\underline{a}_2^{\text{I}}$	$\underline{a}_0^{\text{I}}$	$\underline{a}_1^{\text{II}}$	$\underline{a}_2^{\text{II}}$	$\underline{a}_0^{\text{II}}$
$a^{\text{I}}-b^{\text{II}}, a^{\text{I}}-b^{\text{II}}-E$	1	1	1	$\underline{a}^2$	$\underline{a}$	1
$b^{\text{I}}-c^{\text{II}}, b^{\text{I}}-c^{\text{II}}-E$	$\underline{a}^2$	$\underline{a}$	1	$\underline{a}$	$\underline{a}^2$	1
$c^{\text{I}}-a^{\text{II}}, c^{\text{I}}-a^{\text{II}}-E$	$\underline{a}$	$\underline{a}^2$	1	1	1	1
$a^{\text{I}}-c^{\text{II}}, a^{\text{I}}-c^{\text{II}}-E$	1	1	1	$\underline{a}$	$\underline{a}^2$	1
$b^{\text{I}}-a^{\text{II}}, b^{\text{I}}-a^{\text{II}}-E$	$\underline{a}^2$	$\underline{a}$	1	1	1	1
$c^{\text{I}}-b^{\text{II}}, c^{\text{I}}-b^{\text{II}}-E$	$\underline{a}$	$\underline{a}^2$	1	$\underline{a}^2$	$\underline{a}$	1

$\underline{a} = \exp(j2\pi/3)$ ;  $j = \sqrt{-1}$

Substituting (10) into (9) and taking into account (3)–(8), the following form of the generalized fault-loop model is obtained:

$$(11) \quad \underline{V}_{\text{FL}} - d\underline{Z}_{1L} \underline{I}_{\text{FL}} - R_F \underline{I}_F = 0$$

where:

$$\underline{V}_{\text{FL}} = (\underline{a}_1^{\text{I}} - \underline{a}_1^{\text{II}}) \underline{V}_{S1} + (\underline{a}_2^{\text{I}} - \underline{a}_2^{\text{II}}) \underline{V}_{S2} + (\underline{a}_0^{\text{I}} - \underline{a}_0^{\text{II}}) \underline{V}_{S0},$$

$$\underline{I}_{\text{FL}} = \underline{J}_{12} + \frac{\underline{Z}_{0L}}{\underline{Z}_{1L}} \underline{J}_0 + \frac{\underline{Z}_{0m}}{\underline{Z}_{1L}} \underline{J}_{0m},$$

$$\underline{J}_{12} = (\underline{a}_1^{\text{I}} \underline{I}_{S1}^{\text{I}} - \underline{a}_1^{\text{II}} \underline{I}_{S1}^{\text{II}}) + (\underline{a}_2^{\text{I}} \underline{I}_{S2}^{\text{I}} - \underline{a}_2^{\text{II}} \underline{I}_{S2}^{\text{II}}),$$

$$\underline{J}_0 = \underline{a}_0^{\text{I}} \underline{I}_{S0}^{\text{I}} - \underline{a}_0^{\text{II}} \underline{I}_{S0}^{\text{II}},$$

$$\underline{J}_{0m} = \underline{a}_0^{\text{I}} \underline{I}_{S0}^{\text{II}} - \underline{a}_0^{\text{II}} \underline{I}_{S0}^{\text{I}}.$$

The generalized fault-loop model (11) is of compact form and is applicable for all considered inter-circuit faults. Its application for a particular inter-circuit requires use of the

respective complex number coefficients from Table 2. This is distinctive, that mutual coupling effect (the third component at the right-hand side of the formula for the fault-loop current in (11)) is present regardless earth is involved in an inter-circuit fault or not.

From the generalized fault-loop model (11) one can calculate the fault-loop impedance:

$$(12) \quad \underline{Z}_{\text{FL}} = \frac{\underline{V}_{\text{FL}}}{\underline{I}_{\text{FL}}}$$

which under solid faults ( $R_F \cong 0$ ) is equal to positive-sequence impedance of the faulted line section ( $d\underline{Z}_{1L}$ ). This is identically as for conventional distance relay designed for standard shunt faults.

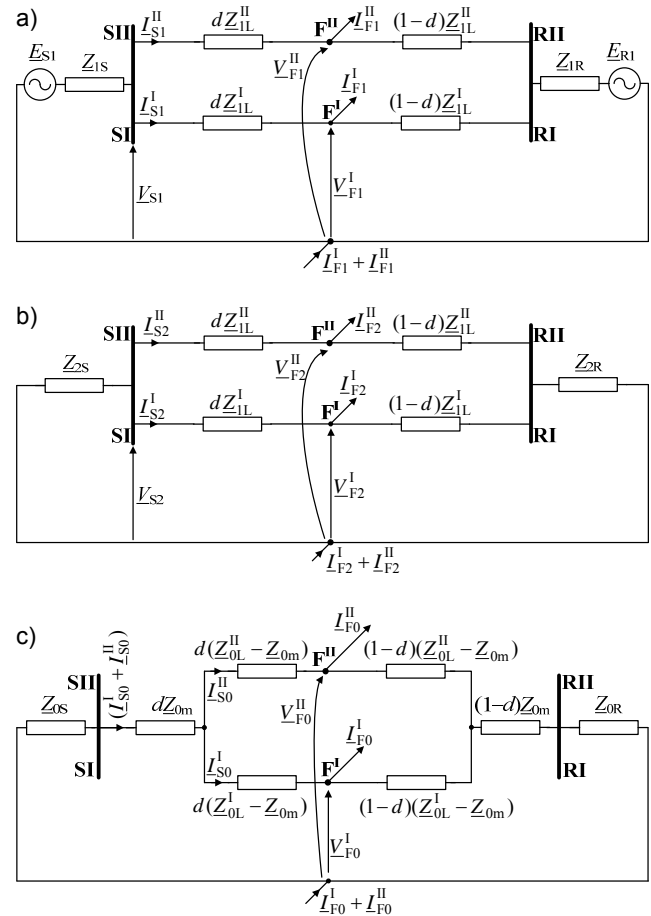


Fig.5. Equivalent circuit diagrams of double-circuit line affected by inter-circuit fault for: a) positive-sequence, b) negative-sequence, c) zero-sequence

### Evaluation of distance protection operation

The distance protection algorithm designed for inter-circuit faults has been tested and evaluated with use of fault data obtained from versatile simulations of faults [18] in a test double-circuit 400 kV, 300 km transmission line. ATP-EMTP software [19] has been applied for that purpose. Selected results of the evaluation study are presented in Figs.6–8 and Table 3.

The line with the following data was modelled:

• impedances:

$$\underline{Z}'_{1L} = (0.0276 + j0.3151) \Omega/\text{km},$$

$$\underline{Z}'_{0L} = (0.275 + j1.0265) \Omega/\text{km},$$

$$\underline{Z}'_{0m} = (0.20 + j0.628) \Omega/\text{km},$$

- shunt capacitances:

$$C'_{1L} = 13.0 \text{ nF/km}, C'_{0L} = 8.5 \text{ nF/km}, C'_{0m} = 5.0 \text{ nF/km}.$$

Equivalent sub-systems behind the line terminals:

- sub-system S:

$$Z_{1SA} = (2.624 + j30.0) \Omega, Z_{0SA} = (4.668 + j53.2) \Omega, \text{ phase angle of phase 'a': } -30^\circ.$$

- sub-system R:

$$Z_{1SB} = 0.5Z_{1SA}, Z_{0SB} = 0.5Z_{0SA}, \text{ phase angle of phase 'a': } 0^\circ.$$

The developed ATP-EMTP model includes voltage and current instrument transformers. Anti-aliasing low-pass analogue filters with a cut-off frequency of 350 Hz were modelled in both current and voltage measurement chains. A/D conversion was performed at 1000 Hz sampling frequency and phasors of the processed signals were determined using full-cycle Fourier filtration [20].

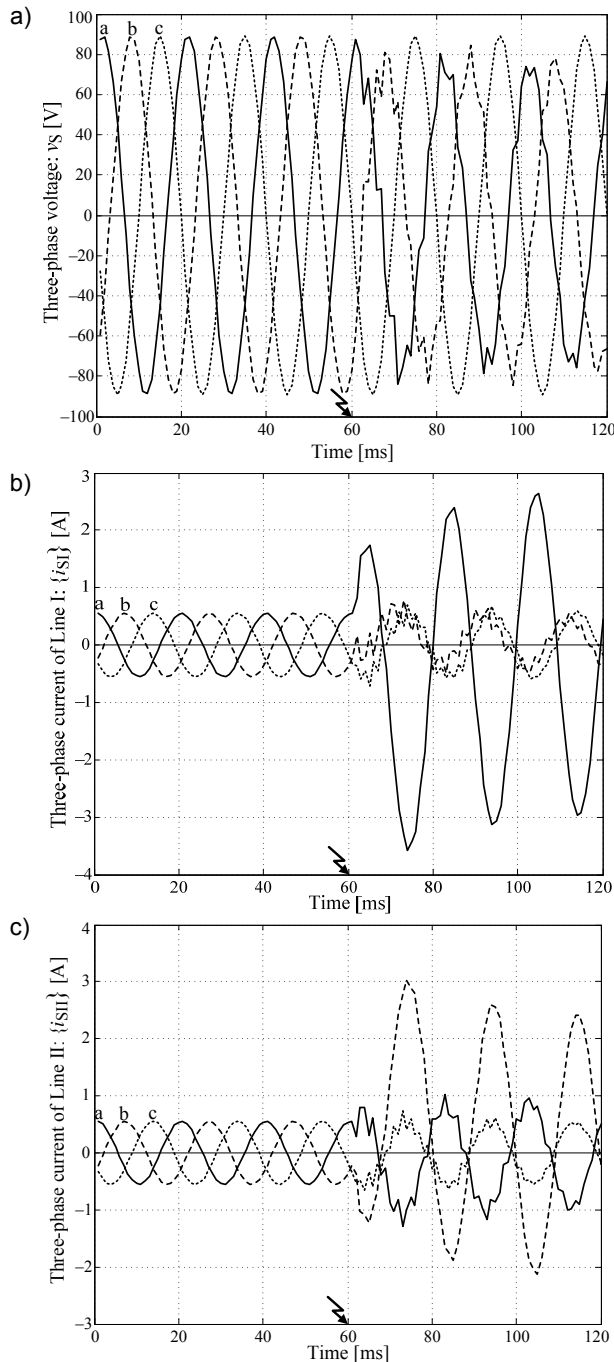


Fig.6. The example – three-phase signals of: a) voltage, b) current from circuit I, c) current from circuit II

The representative example of Figs.6–8 has the following specifications:

- fault type: a<sup>I</sup>–b<sup>II</sup> inter-circuit fault,
- fault resistance:  $R_f = 2 \Omega$ ,
- fault location:  $d = 0.7$  p.u., thus within a reach of a first-zone circle MHO characteristic set in the study at 85%.

Processing the input signals (Fig.6) it has obtained that a fault-loop impedance determined according to the algorithm designed for inter-circuit faults (11)–(12) reliably encroaches the MHO characteristic (Fig.7a). Relay operation (0 – impedance trajectory outside, 1 – inside the MHO characteristic) is presented in Fig.7b. As a result we have required tripping a circuit-breaker of the protected line (for both line circuits).

As opposed to the adaptive distance protection (11)–(12), for a protection designed for standard faults (Table 1) we have a missing operation (Fig.8 – the impedance trajectory remains outside the MHO characteristic).

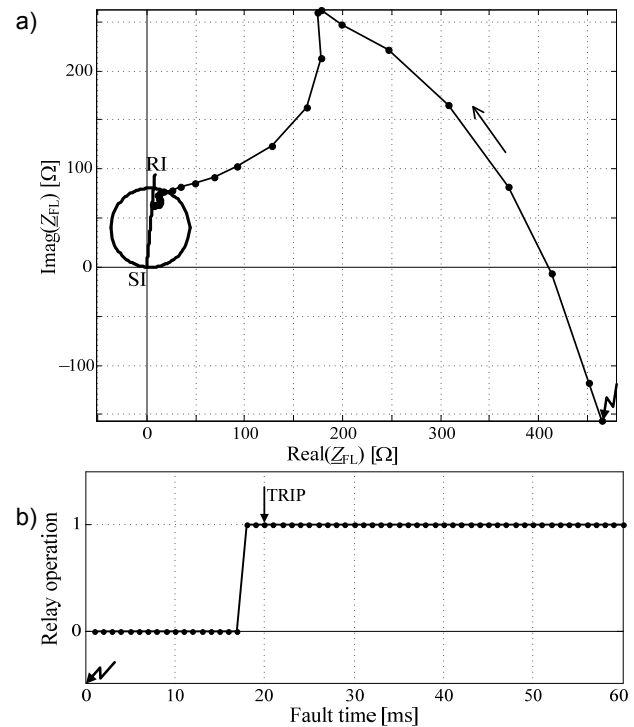


Fig.7. The example – behaviour of distance relay designed for inter-circuit faults: a) trajectory of fault-loop impedance, b) relay operation

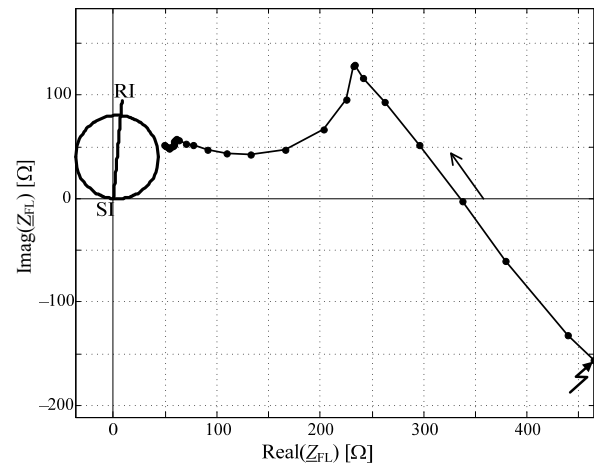


Fig.8. The example – trajectory of fault-loop impedance measured by distance relay designed for standard faults

Besides of correctness of distance relay operation its speed is important for evaluation of protection quality. In the carried study it has been assumed that a relay tripping signal is being issued when for three successive samples a fault-loop impedance trajectory remains inside a relay characteristic (Fig.7).

The inter-circuit fault of the example presented in Figs.7–8 has been taken for further analysis in which a fault location on the line (counted with respect to the buses SI–SII) was varied within the range:  $d = (0.10 \div 0.90)$  p.u. For such series of inter-circuit faults behaviour of the adaptive (11)–(12) and standard (Table 1) distance protection algorithms has been determined and the results are gathered in Table 3. It was performed for the RELAY<sub>S</sub> – installed at the sending line end (at the buses: SI–SII) and the RELAY<sub>R</sub> – from the receiving line end (at the buses: RI–RII). Note that for the relay RELAY<sub>R</sub> from a remote end one has to consider a distance to fault as:  $(1-d)$  [p.u.].

The following results (Table 3) have been obtained:

- RELAY<sub>S</sub>: the reach for the adaptive relay is 85% (as the assumed) while for the standard relay: 60% (thus, considerable shortening),
- RELAY<sub>R</sub>: the reach for the adaptive relay is 80% (shortening by 5% due to negative influence of fault path resistance on impedance measurement) while for the standard relay: 40% (thus, considerable shortening).

Both adaptive relays (RELAY<sub>S</sub> and RELAY<sub>R</sub>) are slightly faster than the standard ones.

Therefore, the adaptive relay exhibits much superior operation than the standard relay. This was also confirmed in the other tests not reported here.

Table 3. Operation of the adaptive and standard distance protection algorithms under a–b<sup>II</sup> inter-circuit faults at different locations

$d$ [p.u.]	Tripping of RELAY <sub>S</sub> [ms]		Tripping of RELAY <sub>R</sub> [ms]	
	Adaptive	Standard	Adaptive	Standard
0.10	13	16	oo	oo
0.15	14	17	xx	xx
0.20	15	17	30	xx
0.25	15	18	28	xx
0.30	16	18	26	xx
0.40	16	20	21	xx
0.50	17	22	19	xx
0.60	18	33	18	31
0.70	20*	xx**	17	21
0.75	22	xx	16	20
0.80	26	xx	16	19
0.85	27	xx	15	18
0.90	oo	oo	14	17

oo – lack of tripping, which is expected

xx – lack of tripping, which is unwanted

\* – see Fig.7b

\*\* – see Fig.8

## Conclusions

New fault-loop impedance measurement algorithm designated for inter-circuit faults on a double-circuit line has been presented. It has been derived with use of a generalized fault-loop model and the obtained formula is compact and applicable for different faults. Complete one-end measurements are required for that. The algorithm is stated in terms of symmetrical components what is also useful for fault location purpose where a compensation for line shunt capacitances is highly required for long lines.

The ATP-EMTP simulation-based evaluation showed much superior operation of the adaptive distance protection equipped with the developed fault-loop impedance measurement over the standard protection in the case of inter-circuit faults on a double-circuit transmission line.

## REFERENCES

- [1] Ziegler G., Numerical Distance Protection. Principles and Applications, *Siemens AG, MCD Verlag*, Erlangen, 2006
- [2] Winkler W., Wiszniewski A., Automatyka zabezpieczeniowa w systemach elektroenergetycznych, *WNT*, Warszawa 1999
- [3] Synal B., Rojewski W., Zabezpieczenia elektroenergetyczne: podstawy, *INPE*, Bełchatów, 2008
- [4] Halinka A., Szabliski M., Wpływ sposobu przyłączania farm wiatrowych do sieci dystrybucyjnej WN na działanie zabezpieczeń odległościowych, *Przegląd Elektrotechniczny (Electrical Review)*, 86 (2010), nr 8, 50–56
- [5] Rebizant W., Solak K., Wpływ nasycania się przekładników prądowych na pracę zabezpieczeń linii przesyłowych, *Przegląd Elektrotechniczny (Electrical Review)*, 86 (2010), nr 11a, 303–307
- [6] Sanaye-Pasand M., Jafarian P., An Adaptive Decision Logic to Enhance Distance Protection of Transmission Lines *IEEE Trans. Power Delivery*, 26 (2011), No. 4, 2134–2144
- [7] Rebizant W., Bejmert D., Improvement of transmission line distance protection with application of fuzzy logic, *Proc. of the CRIS Workshop*, Magdeburg, 2006, 115–120
- [8] Babczyński T., Łukowicz M., Magott J., Selection of Zone 3 time delay for backup distance protection using probabilistic fault trees with time dependencies, *Przegląd Elektrotechniczny (Electrical Review)*, 86(2010), nr 9, 208–215
- [9] Smolarczyk A., Badanie przekładników elektroenergetycznych, *Przegląd Elektrotechniczny (Electrical Review)*, 80(2004), nr 11, 1060–1065
- [10] Izykowski J., Rosołowski E., Saha, M. M., Postfault analysis of operation of distance protective relays of power transmission lines, *IEEE Trans. Power Delivery*, 22 (2007), No. 1, 74–81
- [11] Smolarczyk A., Blokady przeciwkołysaniowe stosowane w zabezpieczeniach odległościowych, *Wiadomości Elektrotechniczne*, 78(2010), nr 10, 21-28
- [12] Gliik K., Rasolomampionona D. D., Kowalik R., Detection, classification and fault location in HV lines using travelling waves, *Przegląd Elektrotechniczny (Electrical Review)*, 88(2012), nr 1a, 269–275
- [13] Szubert K., Wpływ kąta rozchyłu wektorów napięć pomiędzy podsystemami na pomiar impedancji przez zabezpieczenie odległościowe, *Przegląd Elektrotechniczny (Electrical Review)*, 85(2009), nr 4, 173–177
- [14] Makwana V. H., Bhalja B. R., A new adaptive distance relaying scheme for mutually coupled series-compensated parallel transmission lines during inter-circuit faults, *IEEE Trans. Power Delivery*, Vol. 26, NO. 4, October 2011, pp. 2726–2734.
- [15] Makwana V. H., Bhalja B. R., A new adaptive digital distance relaying scheme for double infeed parallel transmission line during inter-circuit faults, *IET Gener., Transm. & Distrib.*, June 2011, Vol. 5 Issue 6, pp. 667–673
- [16] Bachmatiuk A., Distance protection performance under inter-circuit faults on double-circuit transmission lines, *Master's Thesis*, Wrocław University of Technology, Electrical Engineering Faculty, Programme: Master of Science in Electrical Engineering, 2012
- [17] Saha M. M., Izykowski J., Rosołowski E., Fault Location on Power Networks, *Springer*, London, 2010
- [18] Rosołowski E., Komputerowe metody analizy elektromagnetycznych stanów przejściowych, *Oficyna Wydawnicza Politechniki Wrocławskiej*, Wrocław, 2009
- [19] Dommel H.W., Electromagnetic Transients Program, *Manual*, Bonneville Power Administration, Portland, 1986
- [20] Rosołowski E., Cyfrowe przetwarzanie sygnałów w automatyce elektroenergetycznej, *Wydawnictwo Exit*, Warszawa, 2002

**Authors:** mgr inż. Adam Bachmatiuk, Wrocław University of Technology, Electrical Engineering Faculty, E-mail: 159556@student.pwr.wroc.pl; prof. dr hab. inż. Jan Izykowski, Wrocław University of Technology, Institute of Electrical Power Engineering, ul. Wybrzeże St. Wyspiańskiego 27, 50-370 Wrocław, E-mail: jan.izykowski@pwr.wroc.pl.